Composites Part B 312 (2026) 113348

Contents lists available at ScienceDirect

Composites Part B

journal homepage: www.elsevier.com/locate/compositesb

Impact of alkaline exposure and curing environment on mechanical properties of FRCM systems

Matteo Canestri *, Francesca Ferretti, Enrico Sassoni, Claudio Mazzotti

Department of Civil, Chemical, Environmental and Materials Engineering, University of Bologna, Viale Risorgimento 2, 40136, Bologna, Italy

ARTICLE INFO

Keywords:
Durability
Alkaline solutions
FRCM systems
SEM analyses
Basalt and glass fibres

ABSTRACT

Fibre Reinforced Cementitious Matrix (FRCM) systems are widely used retrofitting solutions for strengthening existing structures, offering a high strength-to-weight ratio and excellent compatibility with traditional substrates like masonry. However, the durability of these systems under aggressive environmental conditions remains an open research topic. In particular, the alkaline environment produced by lime-based mortars, used as matrices in FRCM composite materials, might negatively affect the embedded fibres, potentially compromising their long-term performance. This study investigated the durability of two FRCM systems, one incorporating glass fibres and the other basalt fibres, when exposed to alkaline conditions. Textile specimens were immersed in an alkaline solution at two temperatures (23 °C and 40 °C) for a total duration of 1000 h to evaluate fibre degradation. In addition, FRCM coupons were tested to assess the influence of curing conditions and temperature on the tensile performance of the composite system, while mortar prisms cured under identical conditions were tested to characterise the matrix behaviour. To explore the feasibility of accelerated aging protocols, FRCM coupons manufactured using conditioned textiles were also tested. Complementary Scanning Electron Microscopy (SEM) and Energy Dispersive X-ray Spectroscopy (EDS) analyses were performed on both the fibres and their coatings, providing microstructural insights that support the mechanical findings in the tensile tests on textiles.

1. Introduction

In recent years, the use of advanced composite materials has revolutionised structural strengthening techniques, with Fibre Reinforced Cementitious Matrix (FRCM) composites emerging as a cutting-edge solution. They mainly consist of two components: a high strength fabric, usually made of carbon, glass, steel or basalt fibres, embedded inside layers of a cement-, lime-cement- or lime-based mortar matrix. The combination of these two materials creates a strengthening system that is easily applicable and characterised by greater reversibility compared to other types of reinforcements. The structural efficiency of these interventions was already found out by numerous researchers, in particular when applied to masonry components. In more details, many studies focused on analysing the effects of their application on masonry walls to enhance the in-plane and out-of-plane behaviour [1–12]. Similarly, the behaviour of retrofitted curved surfaces such as arches or vaults was also investigated [13–25], while others explained the effectiveness of confinement interventions on masonry columns [26–33]. Since these materials are in most cases applied on the external surfaces of the structural elements, their long-term behaviour under several weathering conditions, such as freeze-thaw cycles, humidity, alkaline or saline environments, remains an unresolved challenge, which definitely needs further research. In recent years, researchers have started investigating the impact of alkaline environments on the performance of FRCM composite systems, by simulating accelerated weathering conditions in a controlled environment. However, the absence of a universally accepted Standard has led to the use of diverse experimental approaches, including differences in pH level, exposure durations, and conditioning temperatures. In two of the earliest studies in the scientific literature [34,35], the impact of an alkaline environment on an alkali-resistant (AR) glass system was examined by altering the chemical composition of the mortar. The results showed that high alkalinity and high temperature (up to 40 °C) might drastically reduce the residual tensile capacity of the AR glass FRCM coupons. In the following studies, a range of different liquid solutions were employed to replicate and simulate an alkaline environment. A solution including Sodium

* Corresponding author.
E-mail addresses: matteo.canestri2@unibo.it (M. Canestri), francesca.ferretti10@unibo.it (F. Ferretti), enrico.sassoni2@unibo.it (E. Sassoni), claudio.mazzotti@unibo.it (C. Mazzotti).

https://doi.org/10.1016/j.compositesb.2025.113348
Received 27 October 2025; Received in revised form 16 December 2025; Accepted 23 December 2025
Available online 24 December 2025

Bicarbonate ($NaHCO_3$) was employed to reach a target pH equal to 10, immerging different specimen types in solutions at 20 °C for a total duration of 1000 h [36,37]. In the first paper [36], tests were performed on a carbon FRCM system, considering conditioned mortar specimens, dry fibres and FRCM coupons. While the mortar matrix appeared to be affected by the ageing protocol, the textile and FRCM coupons, as a whole, were able to preserve 90 % of the total capacity. In the second paper [37], the effect of curing time (28 *vs* 60 days) and exposure were evaluated only on the tensile behaviour of an AR glass FRCM coupons: in general, a strong strength reduction was observed, even if the effect was mitigated in those cases where a longer pre-ageing curing time, in controlled environment, was considered. More aggressive conditioning solutions using NaOH (pH 13–14) showed that exposure time and temperature are critical. Carbon based FRCM coupons retained only 39 % of their strength after 60 days at 40 °C [38]. In another study, various fibres were compared, with AR glass, basalt, and PBO retaining 83–100 % of the capacity, while zinc-coated Ultra-High Strength Steel (UHSS) suffered more significant degradation [39]. Severe strength loss in AR glass fibres was also recorded in high pH solutions [40,41]. Additionally, mixed hydroxide solutions ($Ca(OH)_2$, KOH, NaOH) were used to evaluate the durability of different fibre types over 1000–3000 h of exposure. PBO and carbon fibres demonstrated stability [42], whereas basalt and steel fibres retained only an unsatisfactory 10 % of the initial capacity, with AR glass showing better resilience [43]. Few studies only have systematically compared multiple aging protocols: tensile tests on six fibre types (E-glass, AR-glass, carbon, basalt, PBO, and steel) conditioned under varied temperatures and durations confirmed that basalt and E-glass were the most vulnerable [44]. A second multi-level campaign [45,46] investigated three different conditioning environments and found that AR glass and basalt fibres exhibited substantial performance losses, especially under high-temperature exposure. A recent contribution on basalt FRCM [47] exposed textiles and coupons to $Ca(OH)_2$ solutions at 23–40 °C for up to 3000 h, reporting substantial tensile capacity losses, up to 40–60 % at 40 °C, and confirming the pronounced temperature and alkaline sensitivity of basalt fibres. The same research group investigated also the durability of galvanized SRG systems [48] through direct-tensile, shear-bond and lap-tensile tests after exposure to $Ca(OH)_2$ solutions (pH > 9.5) and alkali soils, showing that while tensile behaviour remained stable up to 3000 h, bond performance was more affected, particularly in lime-based matrices where alkaline ingress was facilitated. A further study [49] assessed long-term conditioning in $Ca(OH)_2$ at pH ≈ 12.6 for up to 5000h, reporting enhanced matrix reactivity but markedly different fibre responses, with glass maintaining or slightly improving bond capacity and basalt experiencing up to 37 % loss. The alkaline durability of Polyphenylene Benzobisoxazole (PBO) FRCM systems was evaluated through direct-tensile tests on coupons immersed in an alkaline solution (pH ≈ 9.5) at 23 °C for 1000 h and 3000 h [50]. The results showed only minor degradation after conditioning, and the authors reported similarly limited effects in a previous study on AR-glass FRCM systems exposed to the same ageing protocol [51]. The most recent investigations focused on natural based FRCM systems, highlighting their marked alkaline sensitivity: direct-tensile tests on aged flax textiles and TRM systems [52] conditioned in $Ca(OH)_2$ for 1000–3000 h revealed progressive stiffness and strength reductions, especially at 40 °C, while complementary tests on coated and uncoated meshes [53] confirmed that suitable surface treatments can limit degradation under $Ca(OH)_2$ exposure. In contrast, NaOH immersion [54] produced substantially more severe deterioration in bare flax textiles, underscoring the higher aggressiveness of sodium hydroxide solutions and the crucial role of fibre coatings and pH level in the long-term performance of flax-based TRM systems. Finally, two preliminary studies conducted by the authors [55,56] further confirmed the detrimental effects of alkaline exposure, showing that prolonged immersion, up to 3000 h, in $Ca(OH)_2$ solutions at 23–40 °C leads to notable tensile capacity losses, with basalt-based FRCM systems experiencing the largest reductions when compared to AR-glass ones. Within the present research activities, two FRCM systems were studied. The experimental protocol followed in this study was aligned with the procedure established by the RILEM Technical Committee 290-IMC *"Round Robin Test on Durability of FRCM"*. First of all, textile specimens were tested after being immersed in solutions of calcium hydroxide ($Ca(OH)_2$) and distilled water at two different temperature levels: 23 °C and 40 °C, for a total of 1000 h. Subsequently, the FRCM coupons were fabricated and cured according to different procedures: first, some FRCM coupons were created with unconditioned textiles and cured in water at both 23 °C and 40 °C or in air, aiming to have reference results and to evaluate the impact of the curing environment; then, with the objective of evaluating possible accelerated conditioning processes, some FRCM coupons were made with textiles conditioned with the mentioned ageing protocol, i.e., alkaline solution at 23 °C or 40 °C for 1000 h, and cured in water at 23 °C for 1000 h prior to testing. At each stage of FRCM coupon preparation, mortar triplets were cast and cured under identical conditions and subsequently tested alongside the FRCM specimens in flexure and compression. The outcomes of all these tests were then compared and analysed and a series of SEM analyses were also conducted to investigate the weathering effects of the conditioning environment on the coating of the bare fibres. Finally, the study aimed to advance the understanding of FRCM durability and the effects of curing environments on their mechanical performance, while representing a significant contribution to the broader experimental programme coordinated under the RILEM TC 290-IMC initiative.

2. Materials and testing methods

2.1. Materials

The FRCM composites investigated in this study were characterised by two different types of fibres as reinforcement and, according to the manufacturer, they had the following characteristics.

- The first system (identified as "S1" in the following) was characterised by a textile made of AR glass fibres, with a weight density equal to 240 g/m^2 and an equivalent thickness of 0.036 mm. This resulted in a cross-sectional area of each bundle equal to 0.9 mm^2. The fibre bundles oriented in the weft direction were slightly flatter and wider than those oriented in the warp direction, with a common grid spacing of 25 mm along the two directions. An organic coating was applied to each individual fibre bundle prior to weaving, resulting in a finished textile where the coated bundles were subsequently interlaced into the final grid pattern (Fig. 1a).
- The second system (identified as "S2") was composed of a basalt textile with a weight density of 304 g/m^2, a grid spacing of 20 mm in each direction and an equivalent thickness of 0.035 mm. The cross-sectional area of each bundle was considered equal to 0.7 mm^2. After being coated with an organic resin, the fibre bundles along the warp direction were thermally connected to the weft ones, without any mutual weaving between the two principal directions (Fig. 1b).

The two systems were completed using different mortar matrices. According to the manufacturers, the mortar used in system S1 was a lime–pozzolanic, cement-free formulation incorporating high-performance polymer (HPF) fibres and fine siliceous aggregates with a maximum size of 0.8 mm. The mix was characterised by high vapour permeability, low capillary absorption, and absence of soluble salts, ensuring compatibility with masonry substrates. The mortar used in system S2 was based on natural hydraulic lime and natural aggregates up to 3 mm, containing only a small fraction of additives (<1 %) and no cement, with similar vapour permeability and chloride content below 0.1 %. The main mechanical properties of the textiles and mortars composing the two FRCM systems, as declared by the manufacturer, were summarised in Table 1.

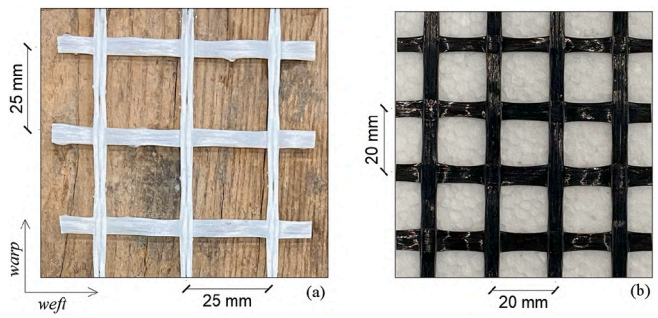

Fig. 1. Textile characteristics: (a) system S1, (b) system S2.

Table 1
– Mechanical properties, as declared by the manufacturers, of textiles and mortars.

Property	System S1	System S2
Textile tensile strength $\sigma_{f,u}$ (MPa)	1600	1496
Textile ultimate strain $\varepsilon_{f,u}$ (%)	2.5	–
Textile elastic modulus E_f (GPa)	65.0	88.7
Mortar compressive strength $f_{m,c}$ (MPa)	>18	>15
Mortar flexural strength $f_{m,fl}$ (MPa)	>4	>4

2.2. Specimens' manufacturing and durability experimental program

In this experimental campaign, different types of specimens were tested, including textiles, mortars and FRCM coupons, in both conditioned and unconditioned states. In order to condition the systems, two alkaline environments were considered, aimed at simulating, in a simplified manner, the alkaline environment produced by the pore solution. To this purpose, distilled water solution containing 0.16 % by weight of calcium hydroxide ($Ca(OH)_2$) was used, a concentration slightly below the solubility limit of $Ca(OH)_2$ in water at room temperature (approximately 0.17 %). This solution was maintained at two controlled temperatures: 23 °C (referred to as C1) and 40 °C (C2).

Firstly, textile strips 460 mm long were cut from the fabric rolls along the warp direction. Each strip included three bundles for system S1 and four bundles for system S2. These strips were then immersed in the alkaline solutions (C1 or C2) for a total duration of 1000 h (Fig. 2a). During this period, the temperature of the solutions was continuously monitored, and the alkalinity level was periodically measured by a conventional pH meter and adjusted accordingly. The average pH values recorded over the entire conditioning duration were 12.4 at 23 °C and 12.1 at 40 °C. At the end of the exposure period, all textile strips were extracted from the conditioning tanks (Fig. 2b). Some of these textiles were directly subjected to tensile tests to evaluate the degradation effects due to the alkaline environment, while others were used as reinforcements in FRCM coupons. In parallel, additional FRCM coupons were also manufactured by using unconditioned textiles, with the aim of isolating the effect of the bare textile deterioration caused by the conditioning environment.

FRCM coupons were produced by first casting a 5 mm layer of mortar into moulds, with a width of 75 mm for system S1 and 80 mm for system S2. The pre-conditioned or unconditioned textile strips were then placed on the fresh mortar surface with precise alignment and parallel positioning within the mould (Fig. 2c). A second layer of mortar, 5 mm thick, was subsequently applied and pressed on top, ensuring full embedding of the textile reinforcement. The resulting FRCM coupon had a final thickness of 10 mm for both systems. After 48 h, the coupons were demoulded and transferred to the curing environments. Curing was performed either in plain water at 23 °C or 40 °C (Fig. 2d), or in air inside a climatic chamber with controlled temperature (23 °C ± 1 °C) and relative humidity (60 % ± 5 %). The duration of the curing phase was 1000 h in all cases. Additionally, mortar prisms with dimensions of 40 × 40 × 160 mm^3 were cast alongside each group of FRCM coupons and subjected to the same curing environments, ensuring identical mortar composition and curing conditions for both prisms and FRCM specimens.

The nomenclature for the specimens followed a structured code system composed of the following parts.

- "S1/S2": identifies one of the two investigated FRCM systems;
- "UN/C1/C2": specifies the textile conditioning regime, i.e., unconditioned, conditioned in an alkaline environment at 23 °C, and conditioned in alkaline environment at 40 °C, respectively;
- "23/40": indicates the curing temperature for FRCM coupons and mortars;
- "A/W": indicates the curing environment for FRCM coupons and mortars (air or water);
- "T/M": final letter indicating either textile (T) or mortar prism (M) specimens.

Table 2 provides a complete overview of all the specimens manufactured and tested during the experimental campaign, including their identification codes, conditioning and curing conditions. For each typology reported in the table, whether textile, mortar or FRCM, five individual specimens were tested.

2.3. Test setups

During the experimental campaign, monotonic tensile tests were conducted on either textile specimens or FRCM coupons, following the indications provided by the European Assessment Document (EAD 340275-00-0104 - annex B and E). At the same time, tests on mortar prisms were conducted following standardised testing method (EN 1015–11:2020), both in flexural and in compression configuration. An example of the adopted setup for all sample typologies is reported in Fig. 3.

The monotonic uniaxial tensile tests on textiles and FRCM specimens were performed by using a servo-hydraulic machine with a 100 kN load capacity, equipped with hydraulic grips. The extremities of the samples were reinforced with FRP tabs in order to ensure an adequate load application to the FRCM coupons, with uniform stress distribution among the individual bundles, and avoiding mortar crushing. All tensile tests were carried out under displacement control, adopting a rate of 0.5 mm/min for textile specimens while two different velocities were employed in the FRCM coupon tests: a rate of 0.2 mm/min in the uncracked stage and 0.5 mm/min in the fully cracked stage. Stress values, for both textiles and FRCMs, were derived dividing the force value by the textile area (2.70 mm^2 and 2.80 mm^2, respectively for systems S1 and S2). In fact, in accordance with standard practice for these materials, stress values in the FRCM coupons were reported in terms of textile stress. On the other hand, strain values were derived from the readings of an extensometer, properly attached to the central region of all specimens. A gauge length of 100 mm was adopted for the textile specimens, whereas it was doubled to 200 mm for the FRCM coupons. On the other hand, tests on mortar prisms were conducted using a three-point bending configuration with a support span of 100 mm. The specimens were tested under load control at a rate of 50 N/s until failure, and the flexural strength was derived from the maximum load recorded. The two fragments resulting from the bending test were subsequently tested in uniaxial compression, loading them between 40 × 40 mm^2 steel plates. The compressive tests were also conducted under load control at a rate of 2400 N/s, in accordance with the standard.

2.4. Microscopic observation and chemical analysis

In order to investigate the effects induced by the conditioning environment on the strengthening system, samples were analysed in top view and cross section by a Scanning Electron Microscope (Tescan Mira

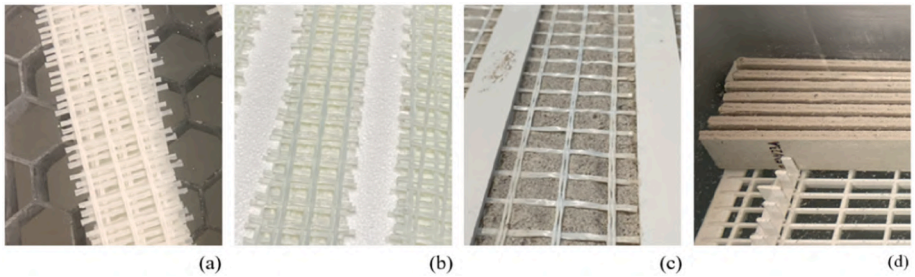

Fig. 2. Example of the manufacturing process of sample S1–C2-23-W: (a) immersion of textile inside the conditioning environment, (b) extraction after 1000 h of exposure, (c) manufacturing of the FRCM coupon and (d) curing stage underwater at 23 °C.

Table 2
Overview of all the specimens tested in the experimental campaign.

Sample type	Specimen ID	Textile conditioning environment[a]	Mortar/composite curing environment
Textile	S1/S2-UN-T	Unconditioned	–
	S1/S2–C1-T	Conditioned AK 23 °C	–
	S1/S2–C2-T	Conditioned AK 40 °C	–
Mortar	S1/S2-23-W-M	–	Water (23 °C)
	S1/S2-40-W-M	–	Water (40 °C)
	S1/S2-23-A-M	–	Air (23 °C)
FRCM coupon	S1/S2-UN-23-W	Unconditioned	Water (23 °C)
	S1/S2-UN-40-W	Unconditioned	Water (40 °C)
	S1/S2-UN-23-A	Unconditioned	Air (23 °C)
	S1/S2–C1-23-W	Conditioned AK 23 °C	Water (23 °C)
	S1/S2–C2-23-W	Conditioned AK 40 °C	Water (23 °C)
	S1/S2–C1-23-A	Conditioned AK 23 °C	Air (23 °C)

[a] AK = alkaline.

3 FEG-SEM), equipped with a Bruker probe for Energy Dispersive X-ray Spectroscopy (EDS) to obtain information on the chemical composition of the analysed samples. In all cases, samples were obtained from the textiles without preliminarily cleaning them. Firstly, samples to be analysed in top view were obtained by cutting a small portion of the textiles at the interweaving of the warp and weft bundles. Secondly, samples to be analysed in cross-section were prepared to analyse the fibre integrity inside the coating along the warp direction. To obtain cross sections, a small portion of textile was cut along the weft direction and then embedded in resin, by placing the textile sample in a plastic mould and pouring the liquid two-component resin. After hardening of the epoxy resin, the embedded samples were demoulded and then the samples to be analysed by SEM were polished to remove excess resin and to expose a flat surface (Fig. 4). Before SEM observation, all the samples were made conductive by sputtering with graphite, and an aluminium bridge was placed over the samples to ensure electric conductivity and electron discharge.

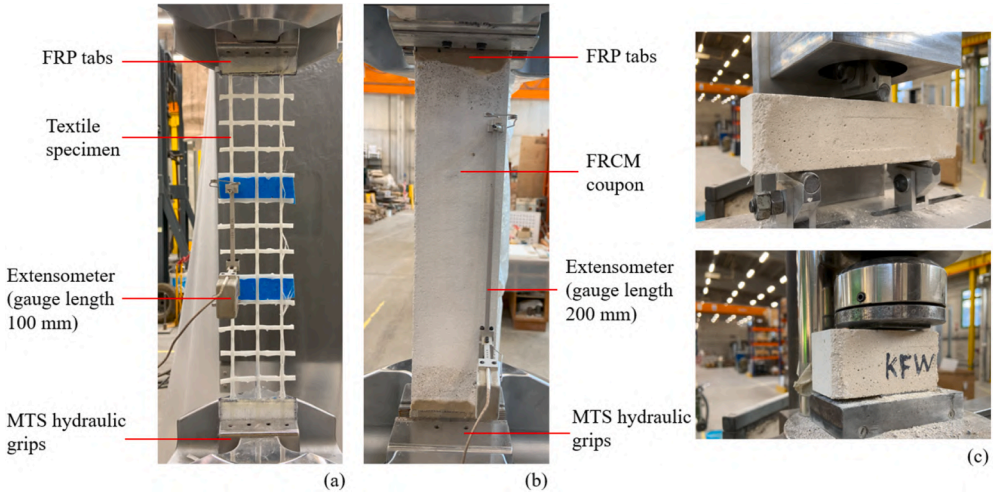

Fig. 3. Setup adopted for tensile tests on (a) textiles and (b) FRCM specimens; setup adopted in flexural and in compression for mortar prisms (c).

Fig. 4. SEM sample preparation: (a) samples to be analysed in top view, (b, c) samples to be analysed in cross section, by embedding them in epoxy resin (b) to obtain the final samples (c).

3. Experimental results

3.1. Textile specimens

Prior to conducting each tensile test, a visual inspection was carried out on both the conditioned and unconditioned textiles. This procedure aimed to evaluate the effects of the alkaline solutions on the integrity of the coating that protects the fibres. For system S1, a minor change in colour was registered, shifting from a semi-transparent coating to a yellow-white one during the exposure period. However, no visible cracks were found (Fig. 5a and b). Conversely, the detrimental effects induced by the conditioning environment on the coating covering the fibres of system S2 were quite evident. In fact, the protective layer appeared to be affected, progressively shifting from a black cleaned reflective surface to a matte one (Fig. 5c and d). Additionally, the surface of the conditioned specimens appeared to be characterised by the formation of multiple cracks.

The experimental results obtained in the tensile tests on textiles are reported in terms of axial stress (σ_f) and strain (ε_f) relationships in Fig. 6. In each graph, the results for unconditioned textiles are shown as solid black lines, while conditioned specimens are represented by dashed lines, differentiated by system (S1 or S2) and conditioning type (C1: 23 °C, C2: 40 °C).

As shown in the graphs, the textiles exhibited a brittle tensile response in all cases, characterised by linear elastic behaviour up to failure, which occurred due to fibre rupture in the central region of the textile specimens. A slight nonlinear phase was observed only in the

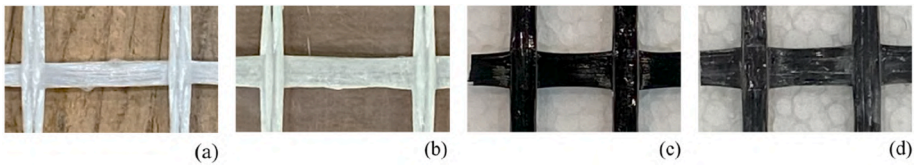

Fig. 5. Alkaline effect on the external coating of fibres: (a) S1-UN-T, (b) SI–C2-T, (c) S2-UN-T, (d) S2–C2-T.

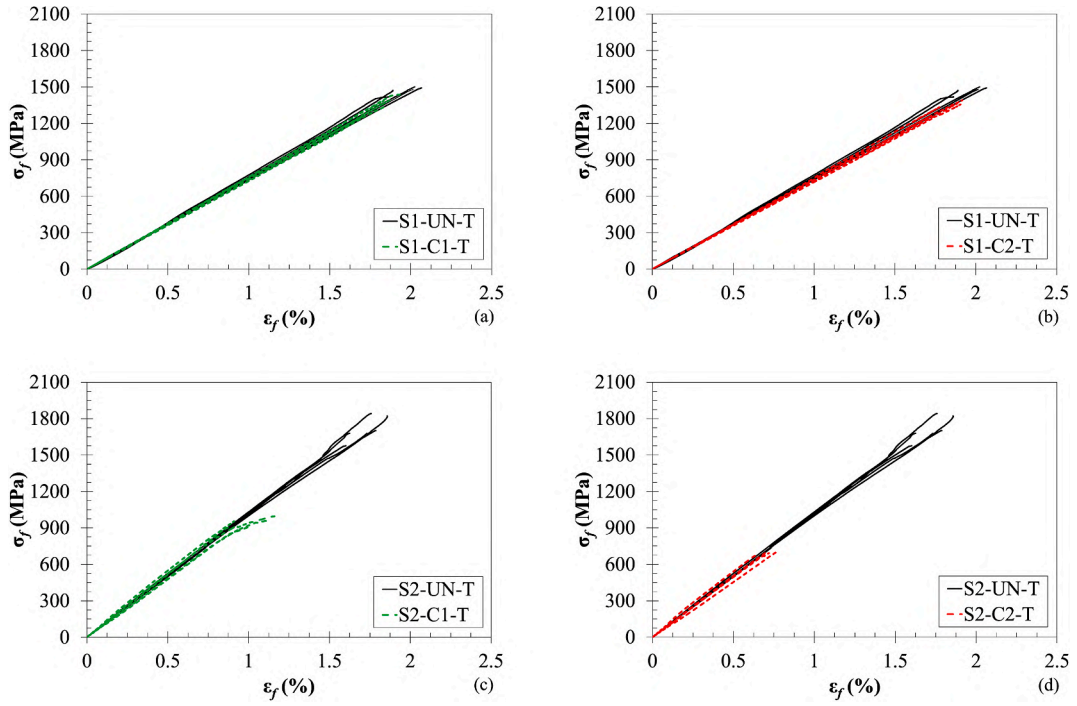

Fig. 6. – Stress *vs* strain curves obtained in tensile tests on textile specimens: (a, b) system S1 samples, unconditioned and conditioned in AK solutions at 23 °C (C1) and 40 °C (C2); (c, d) system S2 samples, unconditioned and conditioned in AK solutions at 23 °C (C1) and 40 °C (C2).

Table 3
Experimental results (average): tensile tests on textile specimens.

Specimen ID	Tensile strength		Ultimate strain		Elastic modulus	
	$\sigma_{f,u}$ (MPa)	CoV $\sigma_{f,u}$ (%)	$\varepsilon_{f,u}$ (%)	CoV $\varepsilon_{f,u}$ (%)	E_f (GPa)	CoV E_f (%)
S1-UN-T	1472	2.2	1.97	4.5	75.6	3.8
S1–C1-T	1369	4.1	1.84	4.1	74.5	1.8
S1–C2-T	1344	3.7	1.85	4.7	73.1	1.6
S2-UN-T	1725	6.3	1.73	6.3	102.4	1.9
S2–C1-T	946	4.2	1.02	12.6	102.2	6.1
S2–C2-T	688	1.8	0.71	6.8	100.7	8.0

curves from specimens of system S1 conditioned in an alkaline environment at 23 °C, near the peak. Additionally, it can be noted that, in all cases, curves were very close together, with minimal dispersion.

Average values of tensile strength ($\sigma_{f,u}$) and ultimate strain ($\varepsilon_{f,u}$) are reported in Table 3, alongside the corresponding coefficients of variation. Elastic moduli (E_f) are listed as well, evaluated as the secant slope of the curves, referring to stress and deformation values between 10 % and 50 % of the peak force. As can be appreciated by the results, almost all CoV were below the 5 % threshold, thus confirming the reliability of the results on textile specimens, with minimal statistical dispersion.

To investigate the effects of alkaline exposure at two distinct temperatures, capacity retention rates (CRR in short) were determined based on the obtained tensile properties and plotted as bar charts in Fig. 7. These rates were calculated by comparing the mechanical performance of conditioned specimens to that of unconditioned reference specimens. The analysis was conducted in accordance with the procedures outlined in ISO 10406-1, using the following equation:

$$CRR_a = \left(\frac{a_{C_1/C_2}}{a_{UN}}\right)\cdot 100 \quad (1)$$

where a_{C_1/C_2} represents the generic average tensile property of the conditioned textile specimens, while a_{UN} represents the average result obtained on the corresponding unconditioned ones.

The results indicate that exposure to an alkaline environment had a negligible effect on the mechanical performance of the dry glass fibres of system S1: high CRRs were observed for all tensile properties under both temperatures of the conditioning solution (23 °C and 40 °C). The slight variations noted fall within the range of experimental scatter, suggesting that the conditioning had no statistically significant impact on system S1. In contrast, the basalt fibre of system S2 exhibited substantial degradation in tensile properties following alkaline exposure. The CRRs for $\sigma_{f,u}$ and $\varepsilon_{f,u}$ decreased markedly, particularly at the elevated conditioning temperature of 40 °C, where strength retention dropped below 40 % and strain retention to 41 %. These results indicate a pronounced susceptibility of basalt fibres to alkaline attack, which is exacerbated by the increased temperature. Interestingly, the elastic modulus remained relatively stable across all conditionings and both systems, with CRRs consistently above 96 %.

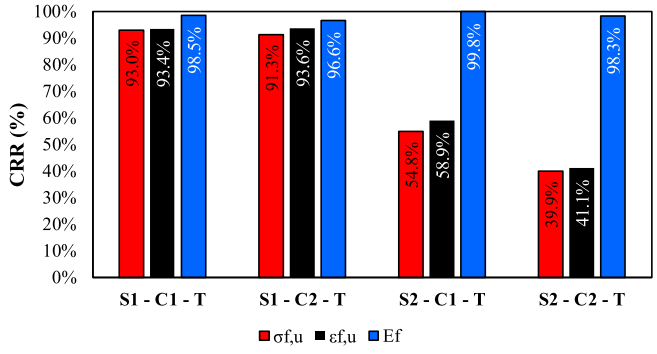

Fig. 7. Capacity retention rates (CRR) of tensile strength, ultimate strain and elastic modulus in tensile tests on textile specimens.

Table 4
Experimental results (average): tests on mortar specimens.

Specimen ID	Flexural strength		Compressive strength	
	$f_{m,fl}$ (MPa)	CoV $f_{m,fl}$ (%)	$f_{m,c}$ (MPa)	CoV $f_{m,c}$ (%)
S1-23-W-M	3.7	11.3	21.1	3.7
S1-40-W-M	4.4	12.0	24.5	1.4
S1-23-A-M	5.5	7.9	25.2	5.7
S2-23-W-M	3.7	7.0	13.3	6.7
S2-40-W-M	3.5	3.9	14.8	5.1
S2-23-A-M	4.1	11.0	15.8	2.4

3.2. Mortar prisms

As previously described, the mortars were cast together with the FRCM coupons and subjected to the same curing conditions as the composite specimens. Specifically, for both systems, mortar prisms were cured in water at controlled temperatures of 23 °C and 40 °C for a total duration of 1000 h. In parallel, additional mortar prisms were cured in air under controlled conditions (23 °C ± 1 °C and relative humidity of 60 % ± 5 %). The results of the flexural and compressive strength tests on the mortars are summarised in Table 4.

The mechanical test results on mortar prisms showed that curing conditions and temperature influenced strength development in both investigated matrices, though with slightly different sensitivities. For both S1 and S2, curing in water at 40 °C led to an increase in compressive strength compared to curing in water at 23 °C, as expected considering that higher temperature generally favours chemical reactions. Curing in air at 23 °C and 60 % RH led to higher compressive strength than curing in water at the same temperature, which can be explained considering that, in water-saturated conditions, CO_2 ingress is blocked, thus hindering carbonation, and lime may be subject to dissolution in water.

In the specific case of the system S1, dispersed HPF fibres are present. According to the technical documentation, these fibres primarily act in the fresh state by reducing plastic shrinkage and influencing moisture distribution. However, their presence also affects the early-age evolution of the matrix when different curing conditions are applied, so that, in the case of air curing, controlled drying promotes carbonation and a more advanced progression of pozzolanic reactions, which favours the development of higher strength.

3.3. FRCM coupons

The results obtained from the direct tensile tests on FRCM coupons are presented in Fig. 8. In particular, for the system S1, Fig. 8a shows axial stress (σ) and strain (ε) relationships for FRCM coupons manufactured with unconditioned textile, cured either in air or water at 23 °C and 40 °C, while Fig. 8b presents axial stress (σ) and strain (ε) relationships for FRCM coupons fabricated with conditioned textiles, cured in air or in water at 23 °C. The same results are reported in Fig. 8c and d for the system S2. Different groups of samples, depending on the conditioning protocol and curing conditions, are distinguished using different colours.

The typical trilinear behaviour was obtained in all tests. In fact, a first stiff linear elastic phase was observed before reaching the first cracking point. Subsequently, the curves showed a small number of stress drops, associated with the formation of additional cracks, finally reaching the third stage of fully cracked behaviour. Table 5 shows the average results for each test group, detailing the maximum tensile strength (σ_u) and ultimate strain (ε_u) at failure, which occurred due to fibre rupture in correspondence with one of the cracks formed in the middle of the FRCM coupon. Subsequently, the third-stage elastic modulus (E_f) was evaluated as the slope of the last branch of the constitutive behaviour, i.e.

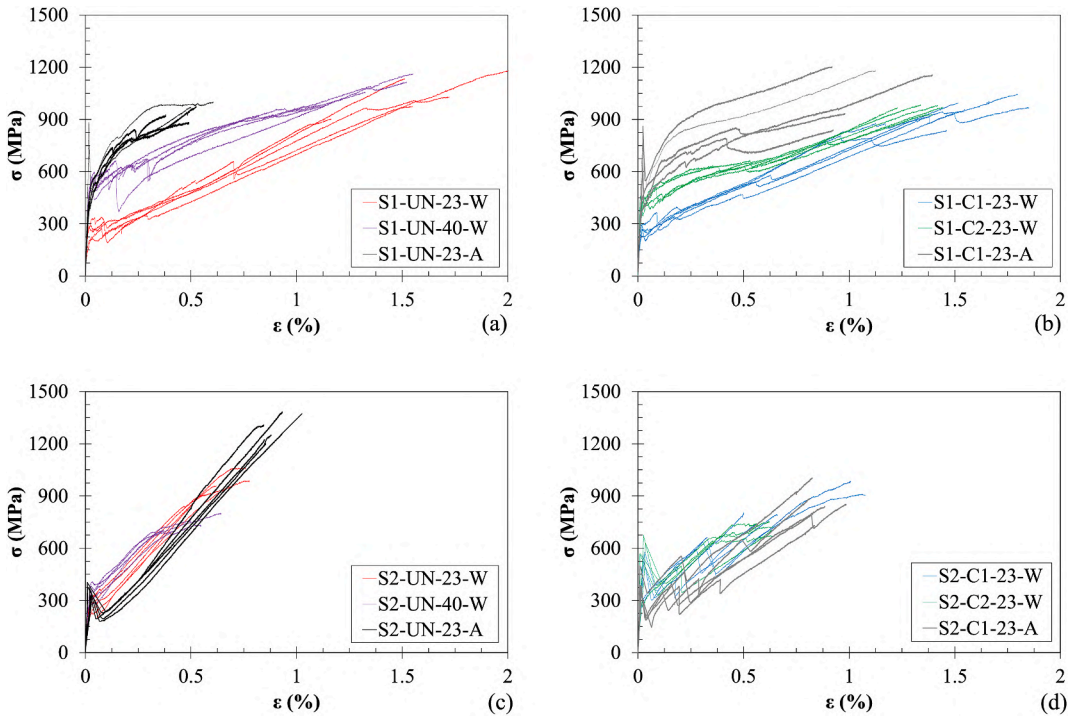

Fig. 8. Stress *vs* strain curves obtained in tensile tests on FRCM coupons: (a, b) system S1; (c, d) system S2.

Table 5
Experimental results (average): tensile tests on FRCM coupons.

Specimen ID	Tensile strength		Ultimate strain		Elastic modulus	
	σ_u (MPa)	CoV σ_u (%)	ε_u (%)	CoV ε_u (%)	E_f (GPa)	CoV E_f (%)
S1-UN-23-W	1046	10.8	1.59	19.4	56.7	14.6
S1-UN-40-W	1061	7.6	1.33	15.7	59.3	16.7
S1-UN-23-A	951	4.9	0.50	16.4	99.2	14.8
S1–C1-23-W	960	8.0	1.63	10.9	51.0	7.8
S1–C2-23-W	967	2.3	1.37	6.3	45.8	15.6
S1–C1-23-A	1063	15.5	1.07	18.6	46.4	8.9
S2-UN-23-W	970	6.2	0.67	13.7	124.3	5.4
S2-UN-40-W	741	5.6	0.51	21.1	116.9	4.3
S2-UN-23-A	1308	5.4	0.91	8.3	124.6	4.0
S2–C1-23-W	847	11.7	0.76	34.8	102.6	7.7
S2–C2-23-W	720	4.4	0.64	1.3	107.7	11.6
S2–C1-23-A	862	11.3	0.82	6.2	115.2	15.1

when the crack propagation process ended.

3.3.1. *Effect of curing conditions on FRCM coupons fabricated with unconditioned textiles*

The initial focus was placed on evaluating how the curing environment affects specimens fabricated with unconditioned textile. In the AR-glass system (S1), air curing at 23 °C (S1-UN-23-A) resulted in a noticeably stiffer overall response, with the highest third stage elastic modulus (E_f = 99.2 GPa) among all conditions, compared to 56.7 GPa and 59.3 GPa for water-cured specimens at 23 °C and 40 °C, respectively (S1-UN-23-W and S1-UN-40-W). This trend is consistent with the results of the mortar tests and suggest that air curing might have enhanced matrix shrinkage and improved early mechanical interlock, increasing stiffness but limiting the overall deformation of the samples. However, the peak stress values remained comparable across the different curing environments, falling within the range of statistical variation of the tests. The influence of the curing environment was much more prominent in system S2 (S2-UN-23-W, S2-UN-40-W and S2-UN-23-A). In fact, contrary to what was observed in system S1, the deformability of the coupons was similar, with comparable elastic modulus in the third stage. However, higher peak stress values were obtained in the samples cured in air, with reduced capacity of the sample cured underwater at 23 °C and 40 °C. To explain this, it should be taken into account that an alkaline environment is inevitably created when immerging mortar inside water, due to the ions release into the pores. This condition significantly reduces the tensile capacity of the embedded basalt fibres, thus making the FRCM coupon highly susceptible to degradation, as previously demonstrated for the tensile tests on textile specimens (Fig. 7). These results highlighted how the interplay between curing conditions and textile type governed the mechanical performance of the FRCM composites. While air curing led to a stiffer response in system S1 without significantly affecting its tensile strength, it notably improved the tensile capacity of system S2 without altering its stiffness. This contrast reflected fundamentally different fiber–matrix interaction mechanisms and underscored the distinct sensitivity of each textile type to environmental curing effects.

3.3.2. *Effect of curing conditions on FRCM coupons fabricated with conditioned textiles*

The analysis then focused on assessing the impact of curing conditions on FRCM coupons incorporating conditioned textiles, by comparing the behaviour of samples cured in water or air at 23 °C. For system S1 (S1–C1-23-W and S1–C1-23-A), the overall tensile response followed a similar trend in both cases. However, air curing led to a slightly stiffer response during the initial (uncracked) stage of loading. This effect diminished in the third stage (post-cracking), where the elastic moduli were similar: E_f equal to 51.0 GPa for the water-cured specimens and 46.4 GPa for the air-cured ones. Tensile strength values

also showed minimal variation between the two conditions, indicating that air curing had negligible influence on the overall performance. The group of specimens S1–C2-23-W, manufactured using textiles conditioned in the hot alkaline environment (C2), exhibited comparable tensile strength and stiffness to the S1–C1-23-W group.

For samples belonging to system S2 (S2–C1-23-W and S2–C1-23-A), curing in air did not enhance the tensile response, in contrast to the results observed in system S2 FRCM coupons manufactured with unconditioned textile. In fact, if a weakened conditioned textile was used for manufacturing the FRCM coupons, the beneficial effects of curing the sample in air was lost due to the presence of an already damaged textile, which governed the tensile behaviour in the cracked stage. For the samples characterised by conditioned textile in the hot alkaline environment (C2) the overall tensile strength was lower compared to the samples conditioned in the alkaline environment at 23 °C (C1), as expected from the results obtained in the tests on textiles. Overall, the differences among samples within each group were minimal, except for S1–C1-23-A, which exhibited a modest dispersion in the post-cracking stage. These findings confirm that when textile degradation is significant, the mechanical performance of FRCM systems is dominated by the residual capacity of the reinforcement, regardless of the curing environment.

3.4. SEM analysis on textiles

The analysis of the samples by SEM-EDS in top view primarily aimed at evaluating the condition of the coating covering the fibres and their chemical composition. In terms of chemical composition (Fig. 9), carbon

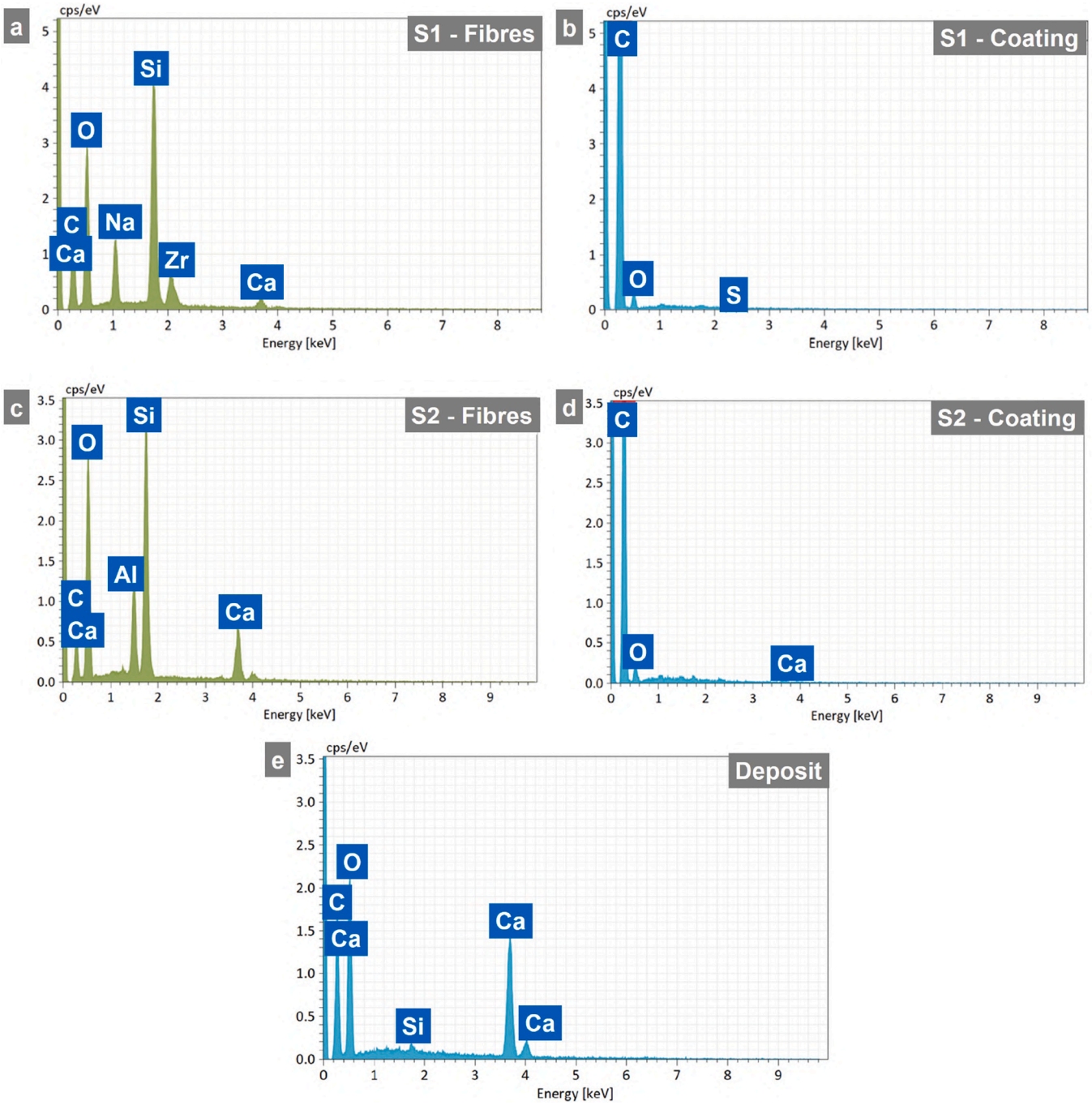

Fig. 9. EDS spectra of: (a) glass fibres and (b) the coating of the system S1; (c) basalt fibres and (d) the coating of the system S2; (e) the deposits in both systems.

was detected by EDS in the coating of both systems (Fig. 9b–d). This is compatible with the coatings being organic in nature (also because of the lack of other strong peaks in the EDS spectra of the coatings), but it should be kept in mind that carbon is also due to the sputtering of the samples with graphite. According to EDS results, glass fibres (system S1 - Fig. 9a) exhibited peaks corresponding to silicon (Si), sodium (Na) and calcium (Ca), as expected, with traces of zirconium (Zr), which is a common additive in fibre compositions designed to enhance resistance in alkaline environments. Basalt fibres (system S2 - Fig. 9c) exhibited peaks of silicon (Si), aluminium (Al), and calcium (Ca), as expected.

From the SEM images related to system S1, it was evident that the unconditioned samples exhibited a continuous and intact surface coating (Fig. 10a), fully covering the glass fibres in both directions, with no signs of cracks or holes. However, exposure to alkaline environments (Fig. 10b and c) for 1000 h led to the formation of small holes and discontinuities in the protective coating. Despite the appearance of these minor defects due to immersion in alkaline media, the overall mechanical strength of the fibres, as shown by the tensile tests, remained unaffected. Moreover, the cross-sectional samples were used to evaluate the state of single internal fibres. The images show that the integrity of the fibre cross section was maintained throughout the conditioning process (Fig. 10d and e), with minimal visible differences, even in samples exposed to elevated temperatures (Fig. 10f).

For system S2, the SEM images revealed that the coating was already compromised in its initial state, displaying multiple clusters of microcracks (Fig. 11a). These areas represented vulnerable points, affecting both the fibres and the organic coating during the conditioning phase. Degradation was evident in the images corresponding to the conditioned samples (Fig. 11b and c). The conditioning process also affected the outer surface of the coating, with several areas characterised by a weathered texture, which was more evident in the sample conditioned at 40 °C. At the same time, the cross section of the fibre was also affected by the aggression of the alkalis permeating the coating, causing a significant reduction of the available effective area and ultimately leading to a reduction in overall capacity, as registered in the tensile tests.

Fig. 12 shows a cross-sectional view of unconditioned and conditioned specimens at a 1000 × magnification, thus offering a broader perspective on the fibre integrity at a larger scale. As evident from the SEM images, the fibres in system S1 remained largely intact, with no significant changes observed in their cross-sectional morphology even after conditioning (Fig. 12a–c). In contrast, the fibres in system S2 appeared intact and uniformly distributed in the unconditioned samples (Fig. 12d), but the alkaline environment, combined with the high temperature of the solution, negatively affected the fibre integrity, thus resulting in noticeable fragmentation of individual elements (Fig. 12e and f).

Finally, it should be noted that in both systems formation of white deposits on the surface of the textiles was visible by naked eye (Fig. 5) and was confirmed by SEM observations (Figs. 10 and 11). EDS analysis of these deposits (Fig. 9e) revealed the presence of calcium (Ca), carbon (C) and oxygen (O) as main elements, which is consistent with the deposits being composed of calcium carbonate ($CaCO_3$). In fact, calcium hydroxide ($CaOH_2$) was dissolved in distilled water to generate the alkaline environment, but most likely it partially reacted with carbon dioxide (CO_2) in the atmosphere also, thus leading to $CaCO_3$ precipitation on the sample surface.

3.5. Comparison with results available in the literature

In this section, the most relevant results from recent research, already discussed in the Introduction, are compared with the new experimental findings presented in this work. Only studies examining the behaviour of basalt or AR-glass FRCM systems under alkaline exposure are here considered, as they directly relate to the materials investigated here. The main outcomes are reported in Table 6 in terms of capacity-retention rates, computed according to Equation (1). This allows assessment of the influence of alkaline conditioning on both tensile strength (at the fibre or FRCM coupon level) and elastic modulus. Since many studies investigated longer conditioning durations, the values reported in Table 6 refer to 1000 h of exposure whenever available, matching the duration adopted in the present study. When 1000 h results were not provided, the closest available value was selected. The literature clearly shows a broad variability in the alkaline solutions used for ageing, both in chemical composition and pH. The reviewed data include results from single-yarn tests, textile tests, and FRCM coupon tests. It is important to clarify that, in the present work, FRCM coupons, fabricated with unconditioned textiles, were not immersed in artificial alkaline solutions but were subjected to water curing, which nonetheless created an alkaline environment for the composite. For this reason, these results are compared with studies that used alkaline-conditioning solutions. It should be also highlighted that it is not trivial to determine which are the reference unconditioned samples to be considered for

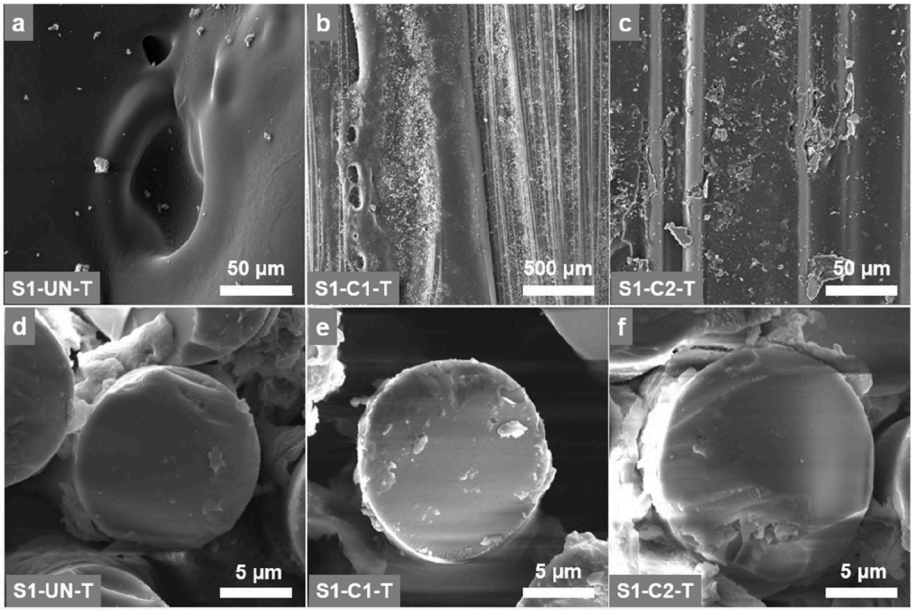

Fig. 10. SEM images in top view (a,b,c) and cross-section (d,e,f) of fibres of unconditioned and conditioned samples (system S1).

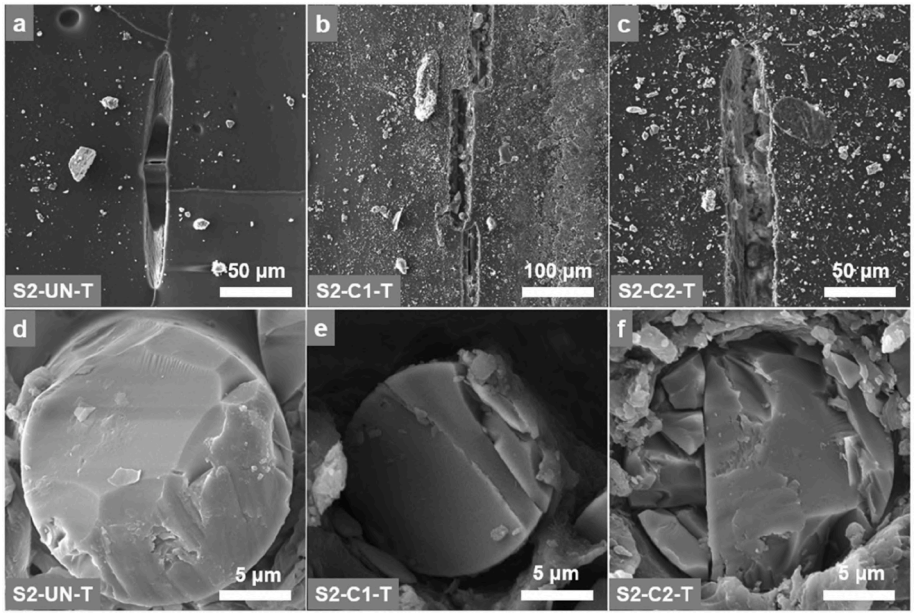

Fig. 11. SEM images in top view (a,b,c) and cross-section (d,e,f) of fibres of unconditioned and conditioned samples (system S2).

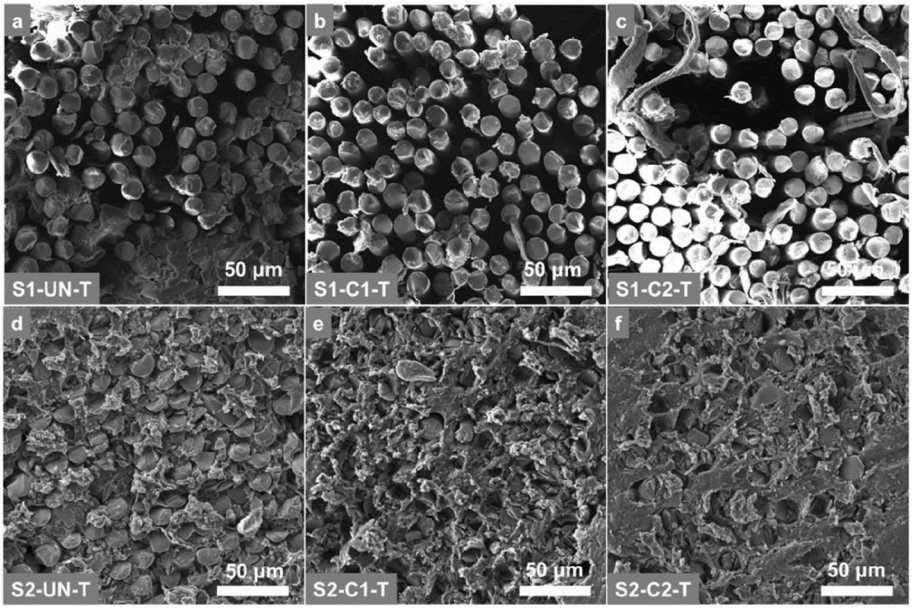

Fig. 12. Cross sectional view at 1000x of fibres of unconditioned and conditioned samples for system S1 (a,b,c) and system S2 (d,e,f).

comparison with results on conditioned samples, and for the calculation of the CRR. Here, the capacity-retention rates for these FRCM coupons were evaluated by comparing specimens cured in water at 23 or 40 °C (S1/S2-UN-23/40-W) with those cured in air (S1/S2-UN-23-A), the latter taken as the reference.

Considering FRCM systems composed by basalt fibres, it is possible to observe a wide variability in terms of capacity-retention rate (CRR) for tensile strength, which seems governed by pH and temperature of the conditioning environment. At textile level, the CRR values vary between 16.0 % and 90.7 %: it is possible to notice that, in general, CRR decreases as the pH value increases, and the lowest results, corresponding to CRR lower than 50 %, are associated with pH values higher than 12 and temperature equal to 40 or 45 °C. For FRCM coupons, higher values of CRR, in the range of 73–82 %, are associated to lower pH values, while under more aggressive environments (pH ≈ 12) the retention rates decrease substantially, with values around 55 %. The results from the present research are consistent with this trend, with tensile-strength CRR values falling within the same range as those observed in Ref. [47], where the same conditioning protocol was adopted, thereby reinforcing the evidence of comparable degradation mechanisms under similar conditioning regimes. Only a limited number of studies report the effect of alkaline exposure on the elastic modulus of basalt fibres and FRCM coupons. In general, for textiles, stiffness is less affected than strength, with CRR values higher than 85 % in all cases; for FRCM coupons a larger variability is observed, which is not clearly correlated with the conditioning environment, but could also be affected by the characteristics of the textile and by the cracking formation and evolution during the tensile tests.

Considering AR glass fibre systems, at textile level, CRR values generally lies between 72 % and 101 %, mainly depending on the value

Table 6
Capacity-retention rates (CRR) from tensile tests on textiles and FRCM coupons: comparison between the available literature and the results of the present study (colour scales are introduced to better highlight the variations of the parameter).

						Yarn or Textile		*FRCM coupons*	
Ref.	Fibre type	Solution	pH	Duration (h)	T (°C)	CRR $\sigma_{f,u}$	CRR E_f	CRR σ_f	CRR E_f
[39]	Basalt	AK2	10	1000	23	-	-	81.9%	-
[43]	Basalt 1	AK3	9.5	1000	23	87.5%	96.3%	76.0%	-
	Basalt 2	AK3	9.5	1000	23	90.7%	95.5%	72.8%	-
[44]	Basalt	AK1	12.6	1440	20	69.0%	-	-	-
	Basalt	AK2	13.5	720	20	54.0%	-	-	-
	Basalt	AK4	12.8	1440	20	65.0%	-	-	-
	Basalt	AK5	12.5	1440	20	58.0%	-	-	-
	Basalt	AK1	12.6	1440	45	52.0%	-	-	-
	Basalt	AK4	12.8	1440	45	16.0%	-	-	-
[47]	Basalt	AK1	12*	1000	23	67.5%	86.3%	54.5%	69.2%
	Basalt	AK1	12*	1000	40	32.9%	88.6%	55.5%	80.6%
This research (system S2)	Basalt	AK1	12.4	1000	23	54.8%	99.8%	74.2%	99.8%
	Basalt	AK1	12.1	1000	40	39.9%	98.3%	56.7%	93.8%
[37]	AR Glass	AK6	10	1000	20	-	-	89.6%	-
[39]	AR Glass	AK2	10	1000	23	-	-	99.4%	-
[41]	AR Glass	AK2	13	1000	40	74.8%	102.6%	101.0%	94.8%
[43]	AR Glass	AK3	9.5	1000	23	101.3%	99.2%	105.8%	-
[44]	AR Glass	AK1	12.6	1440	20	89.0%	-	-	-
	AR Glass	AK2	13.5	720	20	72.0%	-	-	-
	AR Glass	AK4	12.8	1440	20	96.0%	-	-	-
	AR Glass	AK5	12.5	1440	20	100.0%	-	-	-
	AR Glass	AK1	12.6	1440	45	97.0%	-	-	-
	AR Glass	AK4	12.8	1440	45	83.0%	-	-	-
[51]	AR Glass	x	9.5	1000	23	-	-	98.0%	-
This research (system S1)	AR Glass	AK1	12.4	1000	23	93.0%	98.5%	110.0%	57.2%
	AR Glass	AK1	12.1	1000	40	91.3%	96.7%	111.6%	59.8%

Solution	Information about the composition
AK1	0.16% $Ca(OH)_2$
AK2	4 or 5% Na(OH)
AK3	ASTM D7705/D7705M-12
AK4	0.16% $Ca(OH)_2$ + 1% NaOH + 1.4% KOH
AK5	0.2% KOH
AK6	$NaHCO_3$
x / -	Not specified / not obtained

*Information on pH was not reported, the value was assumed based on the characteristics of the solution.

of pH rather than on temperature. At FRCM coupon level, the literature, even if few results are available, and the present research consistently reports high tensile-strength retention, with CRR values higher than 89 % across different solutions and temperatures. The elastic modulus of the textiles remains almost constant and not affected by the conditioning process. For FRCM coupons, instead, the CRR values for the elastic modulus obtained in this research, referring to the fully-cracked stage of tensile tests, are significantly lower than the ones observed for the textile, i.e., in the range of 57–60 %, which is also lower than the value obtained in Ref. [41]. It should be mentioned, however, that the elastic modulus obtained for the samples cured in air (S1-UN-23-A) was remarkably higher than the ones obtained for the system S1 (Table 5), thus influencing the value of the CRR. Given the few available results, it is difficult to draw conclusions, but the difference between the present research and the literature result may be related to the mechanical response of the matrix, affected by the different curing conditions (air/water) for the unconditioned and conditioned FRCM coupons, and the efficiency of the stress transfer within the composite.

4. Conclusions

This research investigated the effects of alkaline exposure and curing environment on the mechanical behaviour and durability of two Fibre Reinforced Cementitious Matrix (FRCM) systems, one reinforced with alkali-resistant (AR) glass fibres and the other with basalt fibres. A conditioning alkaline environment, constituted by a solution of calcium hydroxide and distilled water, was considered. During the experimental campaign, uniaxial tensile tests were performed on different sample typologies: unconditioned and conditioned textiles, FRCM coupons manufactured with unconditioned or conditioned textiles and cured within different environments (i.e., air or water at 23 °C or 40 °C). The results were compared to evaluate the mechanical performance of the

different components of the FRCM systems. Besides the mechanical tests, microstructural changes were analysed by Scanning Electron Microscopy (SEM) and Energy Dispersive X-ray Spectroscopy (EDS).

At the textile level, the study revealed that the glass-based textile of system S1 exhibited good resistance to alkaline degradation, while the basalt-based textile of system S2 showed pronounced deterioration under the same conditions. SEM analysis confirmed, on the one hand, that the AR-glass fibres maintained their structural integrity even after the conditioning process; conversely, SEM images of basalt fibres revealed extensive cracking and deterioration of the protective coating, along with fragmentation of the fibre cross-section.

For FRCM coupons, curing conditions influenced the mechanical behaviour of the samples. On the one hand, water curing resulted in the creation of an alkaline environment due to the composition of the mortar, which negatively affected basalt fibres more than glass ones. On the other hand, air curing showed potential for preserving mechanical properties, especially for FRCM coupons manufactured with unconditioned textiles. When the embedded textile was not sensitive to alkaline exposure, as in system S1, the use of pre-conditioned textiles did not accelerate ageing and led to comparable results to those obtained with unconditioned textiles. Conversely, when the textile was susceptible to alkaline attack, as in system S2, an effect of the water curing as a further conditioning was observed.

Overall, this study contributed valuable data to the growing body of knowledge on the durability of FRCM systems and the results are well aligned with literature, especially for what concerns capacity retention rates values on strength and elastic modulus for textiles. The adopted conditioning protocols, together with the multi-level investigations, were aligned with the procedure established by the RILEM Technical Committee 290-IMC *"Durability of FRCM Systems"*, contributing to the development of a shared testing framework for durability assessment. However, the results obtained could not be automatically extended to all other FRCM systems, as variations in fibre composition and protective coatings may significantly affect the behaviour. It should also be noted that the present study was conducted using a single conditioning duration of 1000 h, which remained relatively short when compared to the design life of structural strengthening interventions. Therefore, future research should include longer conditioning periods and broader environmental exposure scenarios to better assess long-term performance.

CRediT authorship contribution statement

Matteo Canestri: Writing – original draft, Visualization, Methodology, Investigation, Formal analysis. **Francesca Ferretti:** Writing – review & editing, Supervision, Methodology, Conceptualization. **Enrico Sassoni:** Writing – review & editing, Supervision, Investigation, Formal analysis, Conceptualization. **Claudio Mazzotti:** Writing – review & editing, Supervision, Funding acquisition, Conceptualization.

Declaration of competing interest

The authors declare that they have no known competing financial interests or personal relationships that could have appeared to influence the work reported in this paper.

Acknowledgments

The authors would like to express their gratitude for the financial support provided by the Italian Department of Civil Protection through the ReLUIS 2024–2026 Grant (WP14). Special thanks are also extended to the technical staff of the Interdepartmental Centre for Industrial Research (CIRI Buildings & Construction) for their assistance during both manufacturing and testing phases. The authors also gratefully acknowledge the members of the RILEM Technical Committee 290-IMC *"Round Robin Test on Durability of FRCM"* for providing the scientific framework within which this study was developed.

Data availability

Data will be made available on request.

References

[1] Alecci V, Fagone M, Galassi S, Rotunno T, Stipo G, De Stefano M. Experimental shear behaviour of masonry walls reinforced with FRCM. Eng Struct 2024;315:118425. https://doi.org/10.1016/j.engstruct.2024.118425.
[2] Cucuzza R, Domaneschi M, Camata G, Marano GC, Formisano A, Brigante D. FRCM retrofitting techniques for masonry walls: a literature review and some laboratory tests. Procedia Struct Integr 2023;44:2190–7. https://doi.org/10.1016/j.prostr.2023.01.280.
[3] Incerti A, Bellini A, Tilocca AR, Savoia M. Retrofitting with FRCM composites: shear and flexural behaviour of strengthened masonry walls. Key Eng Mater 2022;919:80–9. https://doi.org/10.4028/p-6q01h0.
[4] Meriggi P, Caggegi C, Gabor A, De Felice G. Shear-compression tests on stone masonry walls strengthened with basalt textile reinforced mortar (TRM). Constr Build Mater 2021;316:125804. https://doi.org/10.1016/j.conbuildmat.2021.125804.
[5] Ferretti F, Mazzotti C. FRCM/SRG strengthened masonry in diagonal compression: experimental results and analytical approach proposal. Constr Build Mater 2021;283:122766. https://doi.org/10.1016/j.conbuildmat.2021.122766.
[6] Meriggi P, De Santis S, Fares S, De Felice G. Design of the shear strengthening of masonry walls with fabric reinforced cementitious matrix. Constr Build Mater 2021;279:122452. https://doi.org/10.1016/j.conbuildmat.2021.122452.
[7] Ferretti F, Incerti A, Tilocca AR, Mazzotti C. In-Plane shear behavior of stone masonry panels strengthened through grout injection and fiber reinforced cementitious matrices. Int J Architect Herit 2019;15(10):1375–94. https://doi.org/10.1080/15583058.2019.1675803.
[8] Incerti A, Ferretti F, Mazzotti C. FRCM strengthening systems efficiency on the shear behavior of pre-damaged masonry panels: an experimental study. Journal of Building Pathology and Rehabilitation 2019;4(1). https://doi.org/10.1007/s41024-019-0053-9.
[9] Padalu PKVR, Singh Y, Das S. Out-of-plane flexural behaviour of masonry wallettes strengthened using FRP composites and externally bonded grids: comparative study. Compos B Eng 2019;176:107302. https://doi.org/10.1016/j.compositesb.2019.107302.
[10] D'Ambra C, Lignola GP, Prota A, Fabbrocino F, Sacco E. FRCM strengthening of clay brick walls for out of plane loads. Compos B Eng 2019;174:107050. https://doi.org/10.1016/j.compositesb.2019.107050.
[11] Del Zoppo M, Di Ludovico M, Prota A. Analysis of FRCM and CRM parameters for the in-plane shear strengthening of different URM types. Compos B Eng 2019;171:20–33. https://doi.org/10.1016/j.compositesb.2019.04.020.
[12] Ferretti F, Mazzotti C, Ferracuti B, Tilocca AR. In: In-situ diagonal compression and shear-compression destructive tests on masonry panels from rural buildings in Emilia Romagna region. Proceedings of the 16th international brick and block masonry conference IBMAC; 2016. p. 1553–60. https://doi.org/10.1201/b21889-207.
[13] Kesavan P, Petracca M, Camata G, Sethumadhavan K, Menon A. Discontinuum micromodelling of unstrengthened and FRCM-Strengthened masonry Cross-Vaults subjected to seismic excitation. Int J Architect Herit 2024;18(12):2004–22. https://doi.org/10.1080/15583058.2024.2368637.
[14] Rotunno T, Fagone M, Grande E, Milani G. FRCM-to-masonry bonding behaviour in the case of curved surfaces: experimental investigation. Compos Struct 2023;313:116913. https://doi.org/10.1016/j.compstruct.2023.116913.
[15] Boem I, Gattesco N. Composite Reinforced Mortar (CRM) and Fiber-Reinforced Cementitious Matrix (FRCM) for the seismic protection of masonry vaults. Procedia Struct Integr 2023;44:1260–7. https://doi.org/10.1016/j.prostr.2023.01.162.
[16] Ferrari L, Melegari L. Masonry vaults reinforcement with FRCM-PBO: conservative and structural issues. Key Eng Mater 2022;916:475–82. https://doi.org/10.4028/p-x7hd00.
[17] Misseri G, Stipo G, Galassi S, Rovero L. Bond Behavior of TRM systems and Reinforcement of Masonry arches: testing and Modelling. In: Lecture notes in mechanical engineering; 2020. p. 558–70. https://doi.org/10.1007/978-3-030-41057-5_46.
[18] Kariou FA, Triantafyllou SP, Bournas DA. TRM strengthening of masonry arches: an experimental investigation on the effect of strengthening layout and textile fibre material. Compos B Eng 2019;173:106765. https://doi.org/10.1016/j.compositesb.2019.04.026.
[19] De Santis S, De Felice G, Roscini F. Retrofitting of masonry vaults by basalt Textile-Reinforced mortar overlays. Int J Architect Herit 2019;13(7):1061–77. https://doi.org/10.1080/15583058.2019.1597947.
[20] Scacco J, Milani G, Bove M, Castellano A, Fraddosio A, Piccioni MD. Experimental and numerical analysis of the effectiveness of FRCM strengthening on a parabolic tuff barrel vault. AIP Conf Proc 2019;2186:100005. https://doi.org/10.1063/1.5138011.
[21] Malena M. Closed-form solution to the debonding of mortar based composites on curved substrates. Compos B Eng 2017;139:249–58. https://doi.org/10.1016/j.compositesb.2017.11.044.
[22] De Santis S, Roscini F, De Felice G. Full-scale tests on masonry vaults strengthened with Steel reinforced Grout. Compos B Eng 2017;141:20–36. https://doi.org/10.1016/j.compositesb.2017.12.023.

[23] Alecci V, Misseri G, Rovero L, Stipo G, De Stefano M, Feo L, Luciano R. Experimental investigation on masonry arches strengthened with PBO-FRCM composite. Compos B Eng 2016;100:228–39. https://doi.org/10.1016/j.compositesb.2016.05.063.
[24] Fabbrocino F, Farina I, Berardi VP, Ferreira A, Fraternali F. On the thrust surface of unreinforced and FRP-/FRCM-reinforced masonry domes. Compos B Eng 2015;83:297–305. https://doi.org/10.1016/j.compositesb.2015.08.061.
[25] D'Ambrisi A, Focacci F, Luciano R, Alecci V, De Stefano M. Carbon-FRCM materials for structural upgrade of masonry arch road bridges. Compos B Eng 2015;75:355–66. https://doi.org/10.1016/j.compositesb.2015.01.024.
[26] Campolongo F, Cascardi A, Ombres L. Prediction of the additional compressive strength due to PBO-FRCM-confinement of brick-masonry depending on the stiffening effect caused by different discontinuous wrappings: new design-oriented perspective. Structures 2023;57:105124. https://doi.org/10.1016/j.istruc.2023.105124.
[27] Faleschini F, Toska K. Confinement of masonry columns with FRCM: a new confined strength formulation and experimental validation. Compos Struct 2023;326:117587. https://doi.org/10.1016/j.compstruct.2023.117587.
[28] Alecci V, De Stefano M, Galassi S, Luciano R, Pugliese D, Stipo G. Influence of different mortar matrices on the effectiveness of FRCM composites for confining masonry columns. J Test Eval 2023;51(2):735–50. https://doi.org/10.1520/jte20220323.
[29] Ombres L, Campolongo F, Guglielmi M, Verre S. Experimental analysis of the mechanical response of masonry columns partially confined with PBO FRCM (fabric reinforced cementitious mortar) composites. Materials 2023;16(13):4812. https://doi.org/10.3390/ma16134812.
[30] Canestri M, Ferretti F, Mazzotti C. Confinement of masonry columns through SRG: experimental results and analytical prediction. Procedia Struct Integr 2023;44:2198–205. https://doi.org/10.1016/j.prostr.2023.01.281.
[31] Alecci V, De Stefano M, Galassi S, Magos R, Stipo G. Experimental investigation on the effectiveness of masonry columns confinement using Lime-Based Composite material. In: Lecture notes in networks and systems; 2022. p. 2233–47. https://doi.org/10.1007/978-3-031-06825-6_215.
[32] Aiello M, Bencardino F, Cascardi A, D'Antino T, Fagone M, Frana I, La Mendola L, Lignola G, Mazzotti C, Micelli F, Minafò G, Napoli A, Ombres L, Oddo M, Poggi C, Prota A, Ramaglia G, Ranocchiai G, Realfonzo R, Verre S. Masonry columns confined with fabric reinforced cementitious matrix (FRCM) systems: a round robin test. Constr Build Mater 2021;298:123816. https://doi.org/10.1016/j.conbuildmat.2021.123816.
[33] Minafò G, La Mendola L. Experimental investigation on the effect of mortar grade on the compressive behaviour of FRCM confined masonry columns. Compos B Eng 2018;146:1–12. https://doi.org/10.1016/j.compositesb.2018.03.03.
[34] Butler M, Mechtcherine V, Hempel S. Durability of textile reinforced concrete made with AR glass fibre: effect of the matrix composition. Mater Struct 2010;43(10):1351–68. https://doi.org/10.1617/s11527-010-9586-8.
[35] Butler M, Mechtcherine V, Hempel S. Experimental investigations on the durability of fibre–matrix interfaces in textile-reinforced concrete. Cement Concr Compos 2009;31(4):221–31. https://doi.org/10.1016/j.cemconcomp.2009.02.005.
[36] Nobili A, Signorini C. On the effect of curing time and environmental exposure on impregnated Carbon Fabric Reinforced Cementitious Matrix (CFRCM) composite with design considerations. Compos B Eng 2016;112:300–13. https://doi.org/10.1016/j.compositesb.2016.12.022.
[37] Nobili A. Durability assessment of impregnated Glass Fabric Reinforced Cementitious Matrix (GFRCM) composites in the alkaline and saline environments. Constr Build Mater 2015;105:465–71. https://doi.org/10.1016/j.conbuildmat.2015.12.173.
[38] Signorini C, Nobili A, Falope FO. Mechanical performance and crack pattern analysis of aged Carbon Fabric Cementitious Matrix (CFRCM) composites. Compos Struct 2018;202:1114–20. https://doi.org/10.1016/j.compstruct.2018.05.052.
[39] Signorini C, Nobili A. Comparing durability of steel reinforced grout (SRG) and textile reinforced mortar (TRM) for structural retrofitting. Mater Struct 2021;54(3). https://doi.org/10.1617/s11527-021-01729-3.
[40] Machovec J, Reiterman P. Influence of aggressive environment on the tensile properties of textile reinforced concrete. Acta Polytechnica 2018;58(4):245. https://doi.org/10.14311/AP.2018.58.0245.
[41] Donnini J, Bompadre F, Corinaldesi V. Tensile behavior of a glass FRCM System after different environmental exposures. Processes 2020;8(9):1074. https://doi.org/10.3390/pr8091074.
[42] Arboleda D, Babaeidarabad S, Hays CD, Nanni A. Durability of fabric reinforced cementitious matrix (FRCM) composites. In: 7th international conference on FRP composites in civil engineering, Vancouver; 2014.
[43] Bellini A, Tilocca A, Frana I, Savoia M, Mazzotti C. Environmental durability of FRCM strengthening systems and comparison with dry fabrics. CRC Press eBooks; 2020. p. 370–8. https://doi.org/10.1201/9781003098508-50.
[44] Micelli F, Aiello MA. Residual tensile strength of dry and impregnated reinforcement fibres after exposure to alkaline environments. Compos B Eng 2019;159:490–501. https://doi.org/10.1016/j.compositesb.2017.03.005.
[45] Rizzo V, Bonati A, Micelli F, Leone M, Aiello MA. Influence of alkaline environments on the mechanical properties of FRCM/CRM and their materials. Key Eng Mater 2019;817:195–201. https://doi.org/10.4028/www.scientific.net/kem.817.195.
[46] Micelli F, Rizzo V, Bonati A, Aiello MA. Mechanical behaviour of glass fibers FRCM and CRM systems after ageing in alkaline environments. Key Eng Mater 2022;916:58–65. https://doi.org/10.4028/p-7ztpms.
[47] Fares S, De Santis S, Moretti G, De Felice G. Long-Term Durability of Basalt FRCM in alkaline environment. In: Lecture notes in civil engineering; 2025. p. 587–97. https://doi.org/10.1007/978-3-031-73310-9_41.
[48] Fares S, Meriggi P, De Santis S, De Felice G. Experimental investigation on the tensile and bond durability of galvanized steel reinforced grout. Buildings 2025;15(17):3020. https://doi.org/10.3390/buildings15173020.
[49] Azimi N, Schollbach K, Oliveira DV, Lourenço PB. Effect of exposure to alkaline environment on the mechanical properties of TRM composites. J Build Eng 2025;105:112468. https://doi.org/10.1016/j.jobe.2025.112468.
[50] Calabrese AS, D'Antino T, Colombi P, Poggi C. Long-Term behavior of PBO FRCM and comparison with other inorganic-matrix composites. Materials 2022;15(9):3281. https://doi.org/10.3390/ma15093281.
[51] Calabrese AS, D'Antino T, Colombi P, Poggi C. Durability of a glass fabric-reinforced cementitious matrix composite under different environmental conditions. Key Eng Mater 2022;916:35–42. https://doi.org/10.4028/p-2423m2.
[52] Baldassari M, Trochoutsou N, Monaco A, Cornetti P, Guadagnini M. Tensile response and durability of Flax-TRMs. In: Rilem bookseries; 2024. p. 39–47. https://doi.org/10.1007/978-3-031-70281-5_5.
[53] Tommaso B, Francesca F, Marco P, Claudio M. Effectiveness of different coating treatments on the durability of flax textiles. In: Lecture notes in civil engineering; 2025. p. 69–77. https://doi.org/10.1007/978-3-032-05032-8_6.
[54] Zaydan M, Michel M, Caggegi C, Curtil L. Investigation of the durability of hemp yarns used in textile reinforced mortar (TRM). J Build Eng 2025;113:114178. https://doi.org/10.1016/j.jobe.2025.114178.
[55] Canestri M, Ferretti F, Sassoni E, Mazzotti C. On the behaviour of FRCM fibres in saturated alkaline solution. CRC Press eBooks; 2023. p. 2812–9. https://doi.org/10.1201/9781003323020-342.
[56] Canestri M, Ferretti F, Mazzotti C, Canestri M, Ferretti F, Mazzotti C. Long-Term effects of alkaline environments on basalt fibres. In: Lecture notes in civil engineering; 2025. p. 43–52. https://doi.org/10.1007/978-3-032-05032-8_4.